RESEARCH OF THE IMPLEMENTATION OF A PID ALGORITHM TO CONTROL THE SPEED OF ELECTRIC VEHICLES ON A DYNAMOMETER TEST BENCH

Le Hoang Long[1], Khong Vu Quang[1,*], Pham Huu Nam[2], Pham Van Thoan[3], Pham Minh Hieu[4]

DOI: https://doi.org/10.57001/huih5804.2026.012

ABSTRACT

Evaluating electric vehicle powertrain systems in accordance with regular driving cycles on a dynamometer is a critical necessity; nevertheless, conventional automation techniques frequently incur substantial costs. This paper details the creation and evaluation of an economical automated control system for an electric car powertrain on a test bench. The PID control method is utilized to regulate the speed of a dynamic system employing a permanent magnet synchronous motor (PMSM) in accordance with the WLTC test cycle. This system is programmed on a computer, gets real-time speed readings from the test bench, and directly generates control signals for the motor's power converter. Experimental results demonstrate that the system can precisely monitor the velocity and acceleration attributes of the WLTC cycle, with an average velocity deviation kept below 3.5%. Research has shown that the PID control method is a cost-effective and technically efficient option, offering a viable approach for automating the electric vehicle testing process.

Keywords*: Electric vehicle; Dynamometer test bench; PID; WLTC; PMSM.*

[1]Department of Vehicle and Energy Conversion Engineering, School of Mechanical Engineering, Hanoi University of Science and Technology, Vietnam
[2]Faculty of Mechatronics and Automobile, Hanoi University of Business and Technology, Vietnam
[3]Faculty of Vehicle and Energy Engineering, Phenikaa University, Vietnam
[4]School of Mechanical and Automobile Engineering, Hanoi University of Industry, Vietnam
[*]Email: quang.khongvu@hust.edu.vn
Received: 09/9/2025
Revised: 07/01/2026
Accepted: 28/01/2026

1. INTRODUCTION

The transition from internal combustion engine (ICE) vehicles to electric vehicles (EVs) is essential to tackle global environmental and energy issues. This change substantially aids in reducing greenhouse gas emissions and urban air pollution while simultaneously improving energy security by lessening reliance on fossil fuels. Hence, switching to electrified vehicles signifies a pivotal progression toward a more sustainable future [1]. In a battery electric vehicle (BEV), the electric motor transforms electrical energy stored in the battery to kinetic energy to move the wheels. During deceleration, the traction motor can function to transform a portion of the vehicle's kinetic energy into electrical energy, subsequently stored in the battery. The Regenerative Braking System (RBS) enhances energy economy and augments the vehicle's braking performance through this process [2, 3]. Studies on electric cars, specifically with RBS, mostly concentrates on improving energy conversion efficiency and safety performance [4, 5].

The research and development of an electric vehicle powertrain, encompassing the Regenerative Braking System (RBS), requires multiple tests to assess performance, energy conversion efficiency, and safety. Bench tests are typically performed utilizing standardized driving cycles, like the NEDC (New European Driving Cycle) and WLTC (Worldwide Harmonized Light-duty Vehicles Test Cycle), to provide a comparative framework [6, 7]. Testing systems are generally established in two configurations: Hardware-in-the-Loop (HIL) test benches and dynamometer test benches. P. Fonte et al. [8] employed a Hardware-in-the-Loop (HIL) test bench to evaluate the performance of an electric car powertrain. The test bench was outfitted with a load motor to exert torque on the shaft of the electric motor under examination. The load motor operates according to the outcomes of a computer

simulation of the vehicle's dynamics. Alternative HIL test benches, such those created by R. Schupbach et al. [9] and A. Rassõlkin et al. [10], function on a comparable premise, seeking to minimize the expenses associated with the test bench. The drawback of these test benches is the considerable error in the computer modeling of vehicle dynamics, resulting from the exclusion of several factors present in real-world operating settings.

Dynamometer test benches physically replicate vehicle dynamics through the inertia of rotating masses (rollers) rather than use computer software. This method alleviates the inaccuracies intrinsic to mathematical models of vehicle dynamics. The powertrain can be handled automatically by a device referred to as a pedal robot or robot driver, rather than by manual operation. This device utilizes a combination of electronic, electrical, and pneumatic systems to autonomously regulate the vehicle's accelerator pedal, ensuring compliance with the specified driving cycle velocity. Y. Zhu et al. [11] created a controller for a pedal robot designed for direct installation on the test vehicle. Simultaneously, P. Rautenberg et al. [12] investigated the incorporation of a pedal robot using an autonomous steering mechanism for cars on a test bench. These systems possess intricate construction and control mechanisms, necessitating installation on a physical vehicle, hence significantly elevating testing expenses.

Presently, studies conducted in Vietnam about electric vehicle powertrains, including RBS, are witnessing a significant rising trajectory. D. T. Tung et al. [13] performed research on regenerative braking in relation to driving cycles for hybrid automobiles. Author L. H. Long et al. [14] created a simulation model to assess the energy efficiency of an electric vehicle's dynamics during operation. Nevertheless, the findings of these investigations have solely been validated via computer simulations. In a separate study, L. H. Long et al. [15] evaluated a compact electric car powertrain using a dynamometer to corroborate theoretical simulation outcomes. This research involved mounting just the powertrain components on the test bench rather than the full car, resulting in cost savings. Nonetheless, the evaluations just examined the system's operational attributes during a manual accelerating and braking process, rather than automatically according to a standardized testing cycle. Current dynamometers in Vietnam are engineered for internal combustion engine vehicles; hence, their capacity for cycle-based testing of electric vehicles is constrained.

The PID (Proportional-Integral-Derivative) method is commonly utilized in managing a test or simulation to adhere to a driving cycle. This is a prevalent closed-loop control algorithm in engineering fields, including automotive speed regulation. The PID controller is characterized by straightforward installation and tweaking, superior control quality, and seamless connection with other control algorithms [16]. Consequently, it is an appropriate selection for regulating the speed of an electric car on a dynamometer.

The referenced experimental studies indicate that assessing electric vehicles on dynamometers using standard cycles is essential and offers enhanced physical realism compared to Hardware-in-the-Loop (HIL) testing, which frequently experiences considerable modeling inaccuracies due to the omission of real-world operational variables. Nonetheless, implementing automated cycle-based testing with a pedal robot on a dynamometer poses considerable problems owing to high costs and technical intricacy. Furthermore, the dynamometers presently available in Vietnam are insufficiently engineered for the automatic velocity regulation of electric vehicles. This paper provides an innovative, cost-effective "virtual driver" approach to overcome these limitations. This solution, in contrast to other systems that depend on costly mechanical robot drivers or simulation-intensive Hardware-in-the-Loop (HIL) setups, incorporates the PID algorithm directly into the control software to produce command signals for the motor's power converter. This arrangement obviates the necessity for physical pedal activation while preserving the authentic inertia load of the test bench. This study will elucidate the theoretical and empirical results of applying this PID algorithm to control the testing velocity in alignment with the WLTC. The test subject is an electric car powertrain utilizing a Permanent Magnet Synchronous Motor (PMSM), a common electric motor type for medium to high-power electric vehicles. The experimental velocity and acceleration are juxtaposed with the cycle's parameters to evaluate control effectiveness.

2. FUNDAMENTALS OF CONTROL AND TESTING

2.1. Operating principle of PMSM in electric vehicles

The electric vehicle employs a three-phase wye-connected arrangement for the PMSM, as illustrated in Fig. 1. The rotor encircles the stator in an in-wheel configuration. The PMSM equivalent circuit is analyzed into two components, d and q, as depicted in Fig. 1 [17].

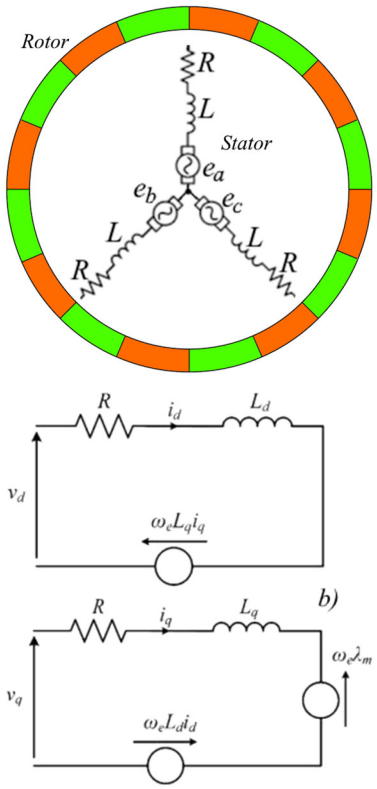

Fig. 1. Operational principle of in-wheel PMSM

The voltage balance of these two components is represented in the equation (1) [17]:

$$\begin{cases} v_d = \left(R + \frac{d}{dt}L_d\right) i_d - \omega_e L_q i_q \\ v_q = \left(R + \frac{d}{dt}L_q\right) i_q + \omega_e L_d i_d + \omega_w \lambda_m \end{cases} \quad (1)$$

For instance, v_d, v_q; i_d, i_q; L_d, L_q; ω_e; λ_m represent the voltages, currents, inductances, electrical angular velocity, and magnetic flux via the motor's stator windings, respectively. The Clark/Park transformation is employed to ascertain the d and q components from phase current and rotor position, as seen in Fig. 2 [18].

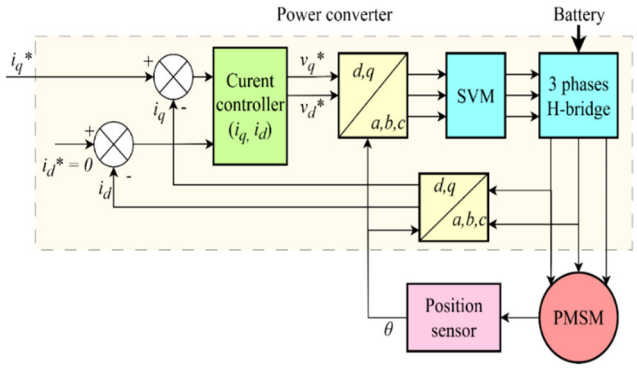

Fig. 2. Power converter for PMSM

The i_d and i_q function as feedback signals for the current intensity controller. The output signals of this controller are the reference voltages v_d^* and v_q^*. The outputs are transformed back into a three-phase electrical signal. According to this signal, the space vector modulator (SVM) and the three-phase current bridge circuit provide power to the PMSM, as illustrated in Fig. 2. The input signal to the power converter is the target current intensity i_q*, derived from the driver's accelerator pedal input.

2.2. Electric vehicle propulsion system under evaluation

The electric vehicle's propulsion system is positioned on a roller-type dynamometer, as seen in Fig. 3. The in-wheel electric motor 1 is affixed to the subframe 4, which is mounted on the main frame 3 of the test bench. The interaction between the wheel and the road is substituted by the interaction between the wheel and roller 2 on the test bench. The load on the wheels is modified by the adjustment mechanism 9. Rotational inertia and surface velocity of the drum supplant the translational inertia and velocity of the vehicle. The power converter 5, battery pack, and electric motor are components of the test vehicle's original propulsion system.

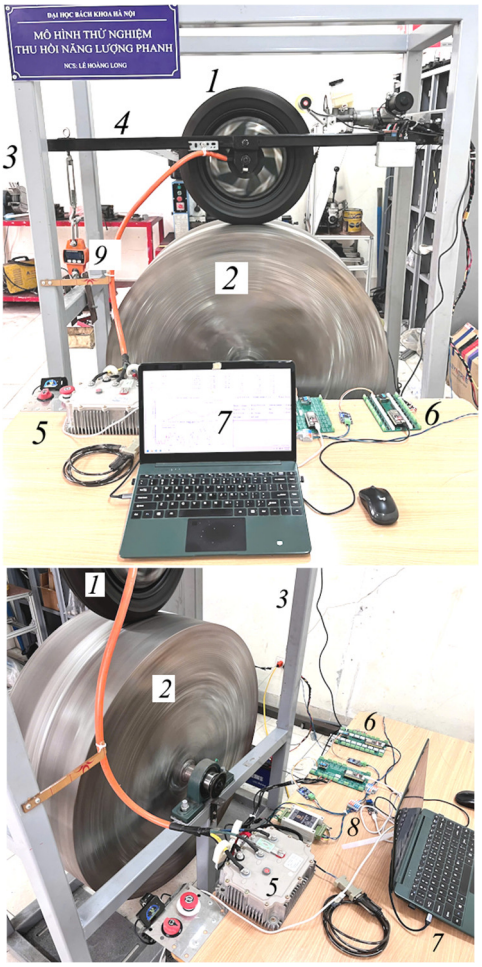

Fig. 3. Configuration of the propulsion and control system of the testing setup

Disregarding the influences of rolling resistance and air resistance, the external forces exerted on the wheel on the test bench are illustrated in Fig. 4. The load *G* applied to the wheel induces a reaction *Z* from the roller, as articulated by the equation (2).

$$Z = G = mg \tag{2}$$

Where *m* represents the equivalent mass applied to the wheel and *g* denotes the acceleration due to gravity.

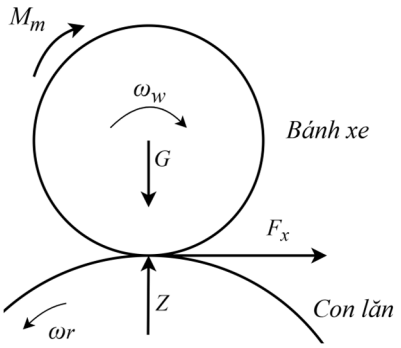

Fig. 4. External force exerted on the wheel on the test bench

The torque produced by the motor, M_m, in conjunction with the adhesion characteristic $\mu(\lambda)$ between the wheel and the roller, results in the longitudinal force F_x, as expressed by the equation (3).

$$F_x = \mu(\lambda)Z \tag{3}$$

The adhesion characteristic $\mu(\lambda)$ is a consequence of the slip ratio λ between the wheel and the roller surface, as delineated in the Pacejka tire model [19]. The slip ratio λ is determined using the equation (4).

$$\lambda = \frac{v - \omega_w r_w}{v} \tag{4}$$

Where, r_w and ω_w are the working radius and angular velocity of the wheel, respectively. *v* represents the velocity at the roller's edge, determined from the roller radius r_r and the angular velocity ω_r as in equation (5).

$$v = \omega_r r_r \tag{5}$$

The angular acceleration of the wheel is determined using the equation (6).

$$\varepsilon = \dot{\omega_w} = \frac{M_m + F_x r_w}{I_w} \tag{6}$$

Where, I_w denotes the moment of inertia of the wheel and electric motor. The car's translational acceleration is substituted by the velocity at the roller's edge as in the equation (7).

$$a = \dot{\omega}_r r_r \tag{7}$$

The angular acceleration $\dot{\omega}_r$ is ascertained by the roller's dynamics via the equation (8).

$$\dot{\omega}_r = \frac{F_x r_w}{I_r} \tag{8}$$

Where, I_r denotes the moment of inertia of the roller. The I_r is computed to ensure that the kinetic energy of the system on the test bench matches that of the vehicle on the road.

2.3. Utilize a speed controller for the test bench

The PID control technique is a widely utilized closed-loop control method in industrial applications, including speed regulation for PMSM [16, 20]. The PID control loop is illustrated in Fig. 5. The goal of the PID controller is to control the output value (test velocity *v*) in accordance with the setpoint (desired velocity v^*).

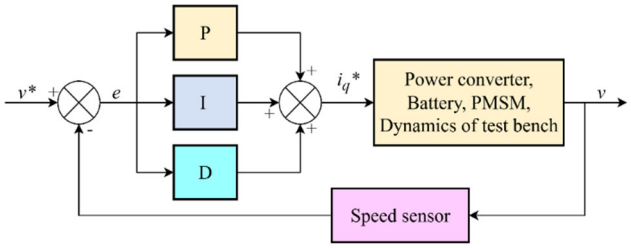

Fig. 5. The control loop of the PID controller

The controller's output signal comprises three components: proportional (P), integral (I), and derivative (D). The components are computed based on the error *e* between the test velocity *v* and the setpoint signal v^* as follows:

$$\begin{aligned} e &= v^* - v \\ P &= K_p e \\ I &= K_i \int e dt \\ D &= K_d \frac{de}{dt} \end{aligned} \tag{9}$$

Where, K_p, K_i, K_d denote the coefficients for the proportional, integral, and derivative components, respectively. The coefficients are modified according to the Ziegler–Nichols method when implemented on the test bench [21]. The ultimate sensitivity strategy was experimentally undertaken to apply this tuning procedure. The controller was initially configured to function exclusively in proportional mode by assigning the integral and derivative coefficients (K_i, K_d) same value of zero (0). The proportional gain K_p was incrementally raised from zero until the system output displayed continuous, prolonged oscillations, signifying minimal stability. At this critical point, the associated proportionate gain was documented as the ultimate gain K_u, and the duration of

these oscillations was quantified as the ultimate period T_u. Utilizing the empirically established critical values, the final K_p, K_i, and K_d parameters were computed according to the usual Ziegler-Nichols tuning methodology. The continuous functions for integration and differentiation in equation (9) are discretized for implementation in a digital processor.

Fig. 3 depicts the elements of the test speed control system, including the measurement apparatus 6, the CAN communication 8, and the computer software 7. This system utilizes sensors to quantify speed, current, and voltage. Fig. 6 depicts the interplay between the elements of the control system and the dynamics on the test bench.

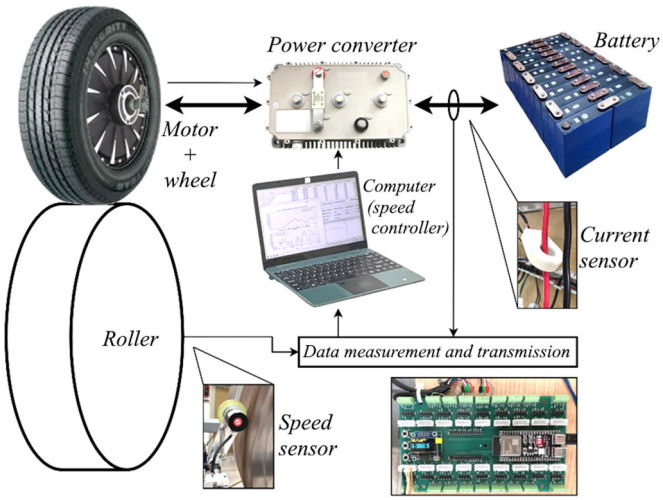

Fig. 6. Signal diagram for testing speed control system

The speed sensor delivers input to the PID controller. Simultaneously, voltage and current sensors function to monitor the operational status of the system. The test velocity was recorded in real-time by computer software utilizing a measuring and data transmission system. The velocity parameters of the test cycle are retained in the computer software's memory and function as the target velocity. The PID algorithm is implemented on a computer. The system functions based on control signals from the computer rather than utilizing signals from the accelerator pedal, brake pedal, and power converter. This enables the system to undergo automatic testing in accordance with test cycles, eliminating the necessity for manual acceleration or brake control.

3. TESTING AND EVALUATING RESULTS

The speed characteristics of the WLTC, Class 3 (Low and Medium), served as the reference signal for assessing the speed control capability of the PID controller. The WLTC is developed according to authentic driving conditions, characterized by continuous variations in speed and acceleration. This cycle is designed to accommodate electric vehicle models.

Throughout the tests, the vehicle's velocity and acceleration metrics were monitored over time to assess its responsiveness and the difference between the tested speed and the desired speed during acceleration and regenerative braking. The discrepancy between the target cycle speed v_{TCi} and the actual vehicle speed v_i is assessed using the average absolute error across n measurements, according to the equation (10).

$$\sigma = \frac{100}{n}\sum_{i=1}^{n}\left|\frac{v_{TCi} - v_i}{v_{TCi}}\right| \ (\%) \tag{10}$$

Where, n is the total count of control loops from the initiation to the conclusion of the test. To provide a more rigorous assessment of the controller's tracking performance and stability beyond the average absolute error, this study incorporates two additional performance indexes: the Maximum Error (E_{max}) and the Root Mean Square Error (RMSE). The Maximum Error identifies the worst-case deviation during transient phases, while the RMSE provides a quadratic mean of the errors, which effectively penalizes large deviations and indicates the overall tracking stability. These metrics are defined as follows:

$$E_{max} = \max|v_{TCi} - v_i|$$
$$RMSE = \sqrt{\frac{1}{n}\sum_{i=1}^{n}(v_{TCi} - v_i)^2} \tag{11}$$

The test parameters for the test bench and the PID controller are presented in Table 1.

Table 1. Specifications of the test bench and PID controller

Parameters	Value
Motor	PMSM QS V3
Maximum power of the motor	9700W @ 900rpm
Maximum torque of the motor	240Nm @ 200rpm
Radius of the wheel	0.23m
Radius of the roller	0.5m
Moment of inertia of the roller	51.25kg.m^2
Equivalent translational mass of the roller	205kg
Battery	LiFePO4 72V, 160A, 50Ah
Speed sensor	Omron E6B2-CWZ6C 1000P/R
Kp; Ki; Kd coefficients	9.5; 0.6; 0.01
Control cycle	50ms
Measurement cycle sample	10ms

The propulsion system's operational variables during WLTC testing have been collected and examined. The experimental velocity was compared with the velocity characteristics of the cycle, as delineated in equation (10) and illustrated in Fig. 7. The discrepancy between the vehicle speed and the cycle's reference speed is $\sigma < 3.5$ %. Occasionally, when the reference speed fluctuates suddenly, delays and overshoots occur, albeit minimally. According to the experimental data gathered throughout the WLTC cycle, the computed error performance indices are are E_{max} = 2.7km/h and *RMSE* = 1.12km/h. The maximum error of 2.7km/h primarily occurs during aggressive deceleration phases ($t = 527$s). This deviation is attributed to the inherent rotational inertia of the dynamometer's rollers, which causes a slight physical lag compared to the rapid reference drop. However, the RMSE value of 1.12km/h is relatively low, confirming that the PID controller maintains tight and stable tracking throughout the majority of the driving cycle, keeping large deviations to a minimum.

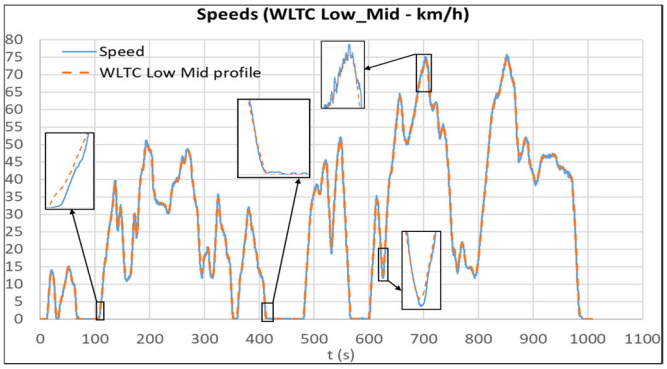

Fig. 7. Measured velocity during testing and the WLTC's velocity profile

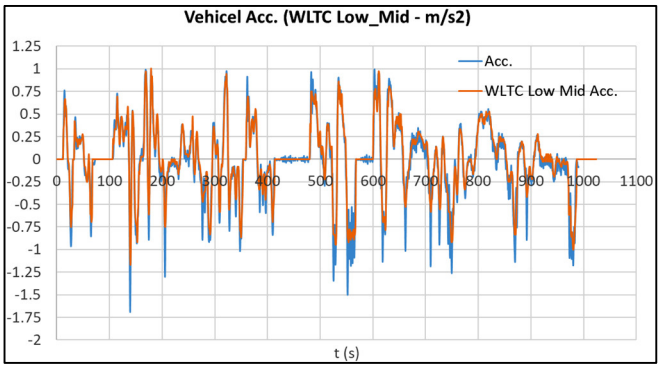

Fig. 8. Acceleration measured during testing and the WLTC acceleration profile

Likewise, the vehicle's acceleration on the test bench almost followed the acceleration characteristics of the test cycle, as illustrated in Fig. 8. The test acceleration fluctuates with a minor amplitude around the cycle's acceleration value during instances of sudden velocity changes. The results indicate that the system put on the test bench performs effectively at acceleration speeds in accordance with the WLTC.

Fig. 8 illustrates the reference braking acceleration in accordance with the WLTC, which generally does not surpass 1m/s². The brake energy recovery system generates braking torque that completely satisfies the necessary deceleration in the cycle. In most urban traffic scenarios (aligned with the WLTC), RBS can execute the braking function independently of the friction braking system.

4. CONCLUSION

The research detailed in the paper has introduced an automated control approach for the testing procedure on a dynamometer for electric vehicles. A PID controller has been effectively implemented in an electric vehicle dynamics system on a test bench, grounded in theoretical principles. The results demonstrate the control system's effective responsiveness in terms of speed and acceleration during the WLTC testing procedure. The discrepancy between the test speed and the desired speed is around 3.5%. Furthermore, the system achieved a RMSE of 1.12km/h, indicating high stability throughout the driving cycle. The maximum error was limited to 2.7km/h, which primarily occurred during rapid deceleration phases due to the inherent inertia of the dynamometer system. This demonstrates that this strategy is effective regarding control characteristics and cost. According to the approach of this study, alternative optimal control algorithms may also be evaluated for implementation in regulating the test velocity.

REFERENCES

[1]. F. Un-Noor, S. Padmanaban, L. Mihet-Popa, M. Mollah, E. Hossain, "A Comprehensive Study of Key Electric Vehicle (EV) Components, Technologies, Challenges, Impacts, and Future Direction of Development," *Energies,* 10, 8, 1217, 2017. DOI: 10.3390/en10081217.

[2]. Y. G. A. E. Mehrdad Ehsani, *Modern Electric, Hybrid Electric, and Fuel Cell Vehicles*. Boca Raton: CRC, 2010. DOI: 10.1201/9781420054002.

[3]. C. Chan, K. Chau, *Modern Electric Vehicle Technology.* Oxford University Press, 2001. DOI: 10.1093/oso/9780198504160.001.0001.

[4]. M. Hannan, M. Hoque, A. Mohamed, A. Ayob, "Review of energy storage systems for electric vehicle applications: Issues and challenges," *Renewable and Sustainable Energy Reviews,* 69, 771-789, 2017. DOI: 10.1016/j.rser.2016.11.171.

[5]. J. A. Sanguesa, V. Torres-Sanz, P. Garrido, F. J. Martinez, J. M. Marquez-Barja, "A review on electric vehicles: Technologies and challenges," *Smart Cities,* 4, 1, 372-404, 2021. DOI: 10.3390/smartcities4010022.

[6]. J. Lasocki, "The WLTC vs NEDC: A Case Study on the Impacts of Driving Cycle on Engine Performance and Fuel Consumption," *International Journal of Automotive and Mechanical Engineering,* 18, 3, 9071-9081, 2021. DOI: http://dx.doi.org/10.15282/ijame.18.3.2021.19.0696.

[7]. L. Sileghem, D. Bosteels, J. May, C. Favre, S. Verhelst, "Analysis of vehicle emission measurements on the new WLTC, the NEDC and the CADC," *Transportation Research Part D: Transport and Environment,* 32, 70-85, 2014. DOI: https://doi.org/10.1016/j.trd.2014.07.008.

[8]. P. Fonte, P. Almeida, R. Luis, R. Pereira, M. Chaves, "Powertrain Test Bench System," in *2019 Electric Vehicles International Conference (EV)*, Bucharest, Romania, 2019. DOI: https://doi.org/10.1109/EV.2019.8892925.

[9]. R. Schupbach, J. Balda, "A versatile laboratory test bench for developing powertrains of electric vehicles," in *Proceedings IEEE 56th Vehicular Technology Conference,* Vancouver, BC, Canada, 2002. DOI: https://doi.org/10.1109/VETECF.2002.1040499.

[10]. A. Rassõlkin, V. Vodovozov, "A test bench to study propulsion drives of electric vehicles," in *2013 International Conference-Workshop Compatibility And Power Electronics*, Ljubljana, Slovenia, 2013. DOI: https://doi.org/10.1109/CPE.2013.6601169.

[11]. Y. Zhu, Z. Fu, Z. Fu, X. Chen, Q. Wu, "Multi-Features Fusion for Fault Diagnosis of Pedal Robot Using Time-Speed Signals," *Sensors,* 19, 1, 163, 2019. DOI: https://doi.org/10.3390/s19010163.

[12]. P. Rautenberg, C. Kurz, M. Gießler, F. Gauterin, "Driving Robot for Reproducible Testing: A Novel Combination of Pedal and Steering Robot on a Steerable Vehicle Test Bench," *Vehicles,* 4, 3, 727-743, 2022. DOI: https://doi.org/10.3390/vehicles4030041.

[13]. D. T. Tung, H. P. Son, H. D. D. Anh, N. Q. Thanh, "Research on Simulation of Regenerative Braking System Based on Actual Driving Cycle," *Journal of Technical Education Science, 18(2),* 2023. https://doi.org/10.54644/jte.76.2023.1271.

[14]. L. H. Long, K. V. Quang, P. H. Nam, L. M. Hieu, "The study of effective regenerative brakes on battery electric vehicles," in *6th International Conference on Engineering Research and Applications - ICERA*, Thainguyen, 2023.

[15]. L. H. Long, K. V. Quang, P. H. Nam, P. V. Thoan, L. T. H. Linh, "Braking energy recovery characteristics of small electric motorcycles," in *The 17th Scientific and Technology Conference on Mechanical Power Engineering*, Hanoi, 2024.

[16]. R. M. Jan, C. S. Tseng, R.J. Liu, "Robust PID control design for permanent magnet synchronous motor: A genetic approach," *Electric Power Systems Research,* 78, 7, 1161-1168, 2008. DOI: https://doi.org/10.1016/j.epsr.2007.09.011.

[17]. K. T. Chau, *Electric Vehicle Machines and Drives: Design, Analysis and Application*. John Wiley & Sons, 2015, DOI: 10.1002/9781118752555.

[18]. A. Emadi, *Advanced Electric Drive Vehicles*. Boca Raton: CRC Press, 2014. DOI: https://doi.org/10.1201/9781315215570.

[19]. H. B. Pacejka, *Tire and Vehicle Dynamics*. Butterworth-Heinemann, 2012. DOI: https://doi.org/10.1016/C2010-0-68548-8.

[20]. H. Wang, S. Xu, H. Hu, "PID Controller for PMSM Speed Control Based on Improved Quantum Genetic Algorithm Optimization," *IEEE Access,* 11, 61091 - 61102, 2023. DOI: https://doi.org/10.1109/ACCESS.2023.3284971.

[21]. K. Åström, T. Hägglund, "Revisiting the Ziegler-Nichols step response method for PID control," *Journal of Process Control,* 14, 6, 635-650, 2004. DOI: https://doi.org/10.1016/j.jprocont.2004.01.002.